

Yang Li*, Jing Wang, Jiaquan Zhang, Changgui Cheng and Zhi Zeng

Deformation and Structure Difference of Steel Droplets during Initial Solidification

DOI 10.1515/htmp-2016-0113

Received June 14, 2016; accepted February 20, 2017

Abstract: The surface quality of slabs is closely related with the initial solidification at very first seconds of molten steel near meniscus in mold during continuous casting. The solidification, structure, and free deformation for given steels have been investigated in droplet experiments by aid of Laser Scanning Confocal Microscope. It is observed that the appearances of solidified shells for high carbon steels and some hyper-peritectic steels with high carbon content show lamellar, while that for other steels show spherical. Convex is formed along the chilling direction for most steels, besides some occasions that concave is formed for high carbon steel at times. The deformation degree decreases gradually in order of hypo-peritectic steel, ultra-low carbon steel, hyper-peritectic steel, low carbon steel, and high carbon steel, which is consistent with the solidification shrinkage in macroscope during continuous casting. Additionally, the microstructure of solidified shell of hypo-peritectic steel is bainite, while that of hyper-peritectic steel is martensite.

Keywords: initial solidification, droplet experiments, solidification modes, hypo-peritectic steel, deformation degree, structure

Introduction

Practice showed that hypo-peritectic steels slabs have the highest susceptibility of surface longitudinal cracking compared to other steels. The surface longitudinal cracks

are closely with uneven growth of initial solidified shell, which is caused by uneven air gap and fluxes filling between solidified shell and mold [1–4]. For hypo-peritectic steels, there is large contraction of solidification and phase transformation in a high and narrow temperature range, leading to very uneven initial solidified shell. In order to determine the solidification behavior characteristics of steel, previous researchers had made many high temperature solidification experiments of steel, including dipping test, submerged split chill tensile experiment, and droplet method [5–8].

The droplet method has the following advantages: (a) observing morphology of solidified shell easily after molten steel droplet placed on a chill plate; (b) reducing effect of gravity and spreading time of small sized sample; (c) ensuring unidirectional solidification and heat transfer of solidified shell bottom under a steep temperature gradient; (d) eliminating a need for a side mold that may hinder free deformation. Dong [5], Niyama [9], Shen [10], etc. studied the deformation of Fe-C alloys droplets, which shows a very strong dependence on carbon content, and two peaks of positive deformation were found as carbon contents come near to 0 and 0.12%. In order to study the initial solidification behavior difference among various steels, the droplet method with a copper chill plate is adopted in this paper.

Experimental method

Based on the previous study, an initial solidification experimental system of steel droplets on copper chill plate is developed shown in Figure 1, in which steel samples can be melted and suspended as droplets, and then the droplets fall down to a copper chill plate at a certain speed.

Major installations and experimental steels

A steel sample weighting about 4 g is melted and suspended in the high-frequency induction heating furnace

***Corresponding author: Yang Li**, The State Key Laboratory of Refractories and Metallurgy, Wuhan University of Science and Technology, Wuhan, China; School of Metallurgical and Ecological Engineering, University of Science and Technology, Beijing 100083, China, E-mail: liyang@wust.edu.cn

Jing Wang: E-mail: wangjingrzd@qq.com, **Jiaquan Zhang:** E-mail: jqzhang@metall.ustb.edu.cn, School of Metallurgical and Ecological Engineering, University of Science and Technology, Beijing 100083, China

Changgui Cheng, The State Key Laboratory of Refractories and Metallurgy, Wuhan University of Science and Technology, Wuhan, China, E-mail: ccghlx@wust.edu.cn

Zhi Zeng, Shougang Research Institute of Technology, Beijing 100043, China, E-mail: zens624@163.com

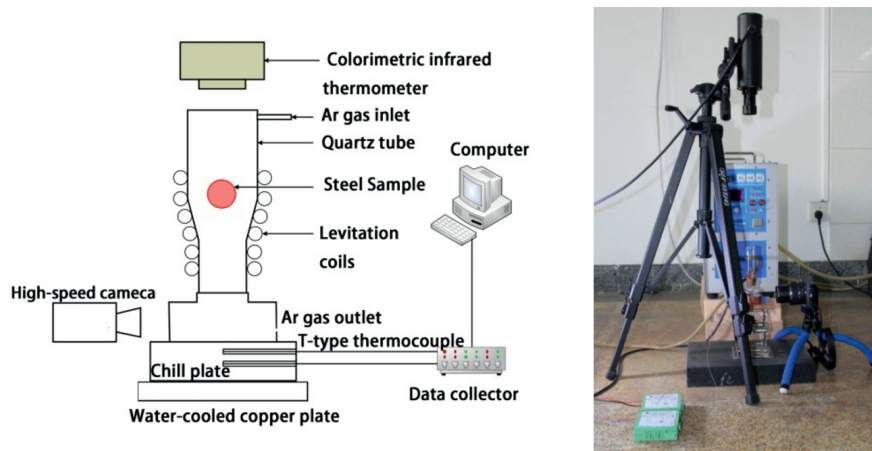


Figure 1: Schematic and whole assembly diagram of initial solidification experiment of steel droplet.

(TX-15A type, maximum power input: 7 kW ; oscillation frequency : 30–100 kHz). This furnace is made of a homemade levitation induction coil and a hollow copper pipe of 3 mm diameter and 0.5 mm thickness. A CIT-1MD type colorimetric infrared thermometer (Beijing Sanbozhongzi Science and Technology Co., LTD), had been used to measure and record upper surface temperature of solidifies shell continuously. T-type thermocouple with high sensitivity at low temperature had been used to rapidly measure the copper plate temperature at the transient instant when the droplet contacts with the plate, and the temperature-time curves had been recorded by a USB7660 type multi-channel temperature sampling instrument. By the aid of Nikon J1 high-speed camera

with frame rate of 400 fps, the deformation of solidified shell in the solidification process on the moment of droplet falling on copper chill plate was observed, and then the time of initial solidification was obtained. The deformation degree and microstructure of solidified shell and surface roughness of copper chill plate was measured by a Laser Scanning Confocal Microscope (Olympus LEXT OLS4000 3D).

The actual composition and carbon equivalent of experimental steels grades is shown in Table 1, including different steel grades according to the calculated results of Factsage software, such as ultra-low carbon (ULC), low carbon (LC), hypo-peritectic(HP), hyper-peritectic(HP*),and high carbon(HC). Firstly, the

Table 1: Actual composition and carbon equivalent content of test steel grades in different solidification modes, mass%.

Steel grade 种	Ceq	C	Si	Mn	Al	Ca	Nb	Ti	V	Cu	Cr	Ni	Mo
ULC1 IF	0.0045	0.0061	0.0037	0.13	0.027	0.0001	0.001	0.07	0.004	0.01	0.01		
LC1 SPHC	0.025	0.028	0.02	0.2	0.033	0.0015	0.001	0.01	0.01	0.0002			
LC2 MR-T2.5	0.052	0.0514	0.02	0.25	0.03	0.0001	0.001	0.01	0.01	0.00001			
LC3 X80	0.089	0.054	0.2	1.83	0.039	0.0021	0.078	0.016	0.023	0.2	0.02	0.21	
HP1 X65	0.102	0.082	0.2	1.55	0.043	0.0025	0.06	0.018	0.019	0.01	0.23	0.01	
HP2 Q550E	0.111	0.086	0.25	1.82	0.032	0.0011	0.037	0.01	0.047	0.02	0.03	0.01	0.002
HP3 S420CL	0.116	0.097	0.1	1.2	0.037	0.0012	0.0009	0.0009	0.00001	0.01	0.02	0.01	
HP4 510L	0.116	0.098	0.1	1.16	0.035	0.0022	0.03	0.0006	0.00001	0.01	0.02	0.01	
HP5 L290	0.155	0.137	0.1	1	0.033	0.0015	0.002	0.017	0.004	0.01	0.02	0.01	
HP6 SS400	0.154	0.154	0.11	0.37	0.022	0.0019	0.001	0.001	0.001	0.01	0.01	0.0048	
HP*1 Q235D	0.170	0.176	0.22	0.74	0.044					0.06	0.16	0.03	
HP*2 26CrMo	0.259	0.276	0.27	1.13	0.008			0.04		0.07	0.86		0.18
HP*3 35CrMo	0.333	0.36	0.27	0.55						0.1	0.95	0.15	0.21
HP*4 45	0.429	0.433	0.27	0.65						0.125	0.125	0.075	0.15
HP*5 50Mn	0.505	0.514	0.27	0.85						0.1	0.125	0.075	0.15
HC1 82B	0.858	0.82	0.217	0.743	0.0028	0.0026	0.0035	0.0024	0.0061	0.0081	0.2373	0.0981	0.0017

steel samples which were from continuously cast strands and machined to a 9 mm diameter rod, were put into the transparent quartz tube around solenoid with Argon gas (3 L/min). The molten steel would drop on the copper chill plate at a target temperature tested by the colorimetric thermometer. The free deformation process of droplet was recorded by high speed camera, while the temperature change of chill plate at instant contact with molten steel was also recorded by the multi-channel temperature sampling instrument. Then the deformation and structure of solidified shell is observed by laser scanning confocal microscope.

Temperature measurement method of copper chill plate

In order to study the initial solidification of various steels, red copper which is the same with mold's material is selected to make the chill plate, with a circular shape of 20 mm in diameter, 15 mm in thickness and 0.026 μm in surface roughness. In order to measure the change of heat flux of copper plate in the initial solidification process, the traditional temperature measurement method which measures temperature with directly thermocouple head was improved based on Todoroki's [11] method. The constantan wire (negative electrode) of T-type thermocouple was inserted into the center of chill plate 2 mm and 4 mm below the upper surface through a 1 mm horizontal hole, while the copper wire (positive electrode) was connected on the copper plate side, shown in Figure 2. Since the material of copper plate is the same as that of positive electrode of T-type thermocouple, there is a current in the case of no welding thermocouple. This method could eliminate the measurement delay of temperature due to the thermocouple welding head, and the temperature change of copper plate at instant contact with molten steel could be measured to study the heat change between droplet and copper plate in a short period of time.



Figure 2: Diagram of temperature measure method on the copper plate.

The temperature curves of T_1 and T_2 of IF steel were respectively measured by traditional temperature measurement

method and modified method, shown in Figure 3. It is shown that the T_1 and T_2 temperatures measured by traditional temperature measurement method increase slowly during 0 to 2 s, whereas, that measured by modified method increases to the peak at about 0.2 s then decreases. Because of the great hysteresis of traditional temperature measurement method, the modified method is adopted in this study to accurately and sensitively measure the temperature change of copper plate at instant contact.

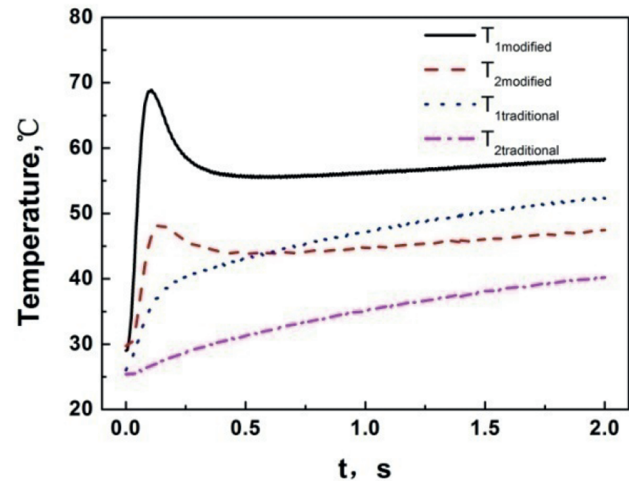


Figure 3: Temperature curves measured by traditional and modified methods.

Index of deformation degree of solidified shell

The shape and bottom profile of center section of solidified shell of S420CL steel was measured by a Laser Scanning Confocal Microscope, shown in Figure 4. It is observed that bottom profile of center section of the solidified shell is a parabola. The bigger curvature value (κ) means the bigger degree of curvature of curve. The maximum curvature of measured parabola was selected as the index of deformation degree of the solidified shell in the experiments. The calculation formula of curvature k is shown in Formula(1), and the fitting formula of parabolic in shell bottom is shown in Formula(2), the calculation formula of maximum curvature k is shown in Formula(3).

$$\kappa = \left| \frac{y''}{(1+y')^{\frac{3}{2}}} \right| \quad (1)$$

$$y = ax^2 + bx + c \quad (2)$$

$$\kappa_{\max} = 2|a| \quad (3)$$

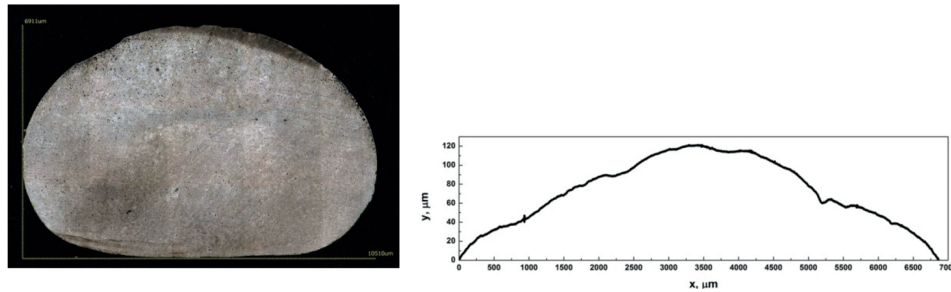


Figure 4: Shape and bottom profile of center section of solidified shell of hypo-peritectic steel.

Choice of testing parameters

In order to choose the reasonable weight of samples to study initial solidification of various steels, 510 L steel samples were processed into cylinder sample with different weights. Samples with different weights dropped on the copper chill plate (burnished) under the condition of same superheat, and the bottom deformation of solidified shell were measured, shown in Figure 5. It's shown that the lower curvature of solidified shell bottom with increased weight of samples, which is in conformity with Dong's [9] experiment results. Take consideration of the differences of deformation and difficulty of bottom curvature measurement, steel samples were processed into cylinder sample ($\Phi 9 \text{ mm} \times 8 \text{ mm}$, weighing 4 g) in this experiment.

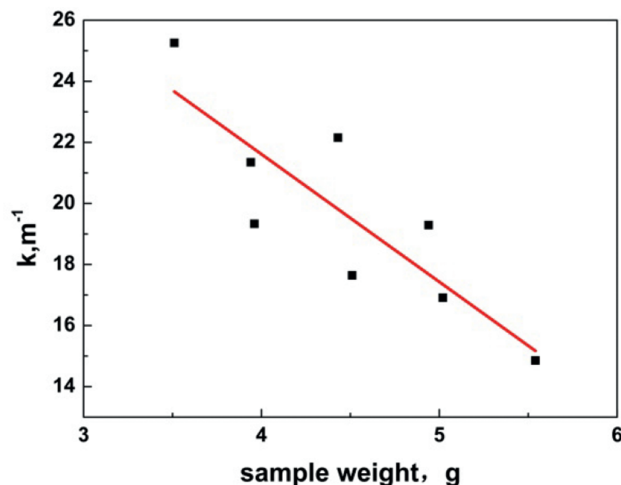


Figure 5: Effect of sample weight on the bottom curvature of solidified shell of 510 L steel grade.

35CrMo hyper-peritectic steel grade was chosen to test the reasonable superheat in the initial solidification experiments. The effect of superheat on the bottom curvature of solidified shell of 35CrMo steel grade is shown in Figure 6. It is shown that the curvature of solidified shell

bottom decreased linearly with increased superheat. This is because the temperature difference of molten steel (T_L) and copper plate surface (T_0) is smaller with the higher molten steel superheat, leading to the decrease of thermal stress and deformation degree of solidified shell. Take according to better observation of differences of deformation degree of solidified shell and the actual superheat of molten steel in mold, the superheat of molten steel was in the range of 10–30 °C in the initial solidification experiments.

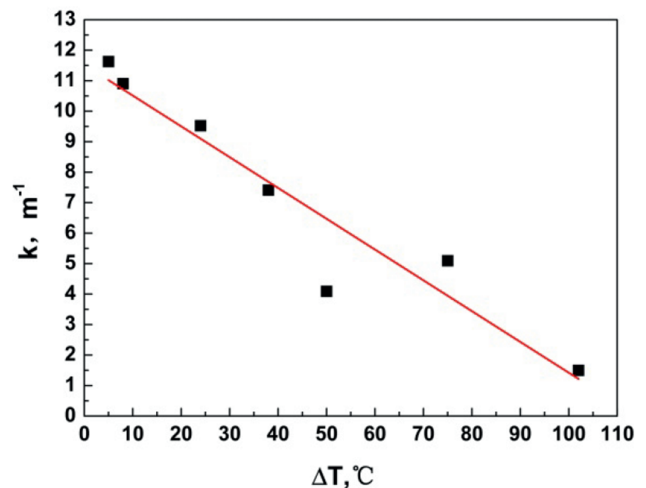


Figure 6: Effect of superheat on the bottom curvature of solidified shell of 35CrMo steel grade.

Experimental results

Difference of solidification and deformation of various steels

The solidification and deformation of various steels at instant contact of steel droplet and the chill plate was recorded by high-speed camera, as shown in Figure 7. And the changes of diameter and thickness of solidified

shell over time during the above solidification and deformation processes were shown in Figure 8. Set the just contact time of steel droplet and the chill plate to 0 ms. It is shown that the droplets of different steels begin to spread out after the contact, and completely spread to maximum diameter at the time of about 9 ms. Then the diameter of bottom solidified shell gradually decreases, and the thickness of solidified shell increases. Finally, the solidified shell remains in a shape with a fixed bottom diameter and thickness. By comparison, the deformation time of solidified shell of IF ultra-low carbon steel and 510 L hypo-peritectic steel was relatively longer than other steel grades. During the solidification of molten steel, the maximum bottom diameters of hypo-peritectic steels (510 L steel and SS400 steel) are largest among all the steels adopted in this experiment. After the deformation of solidified shell, the bottom diameters of solidified

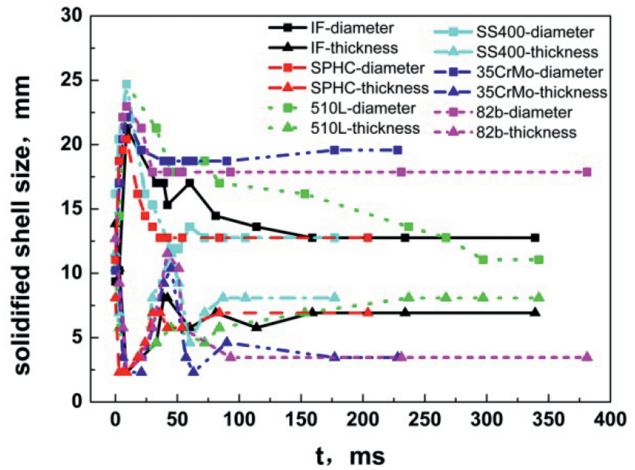


Figure 8: Diameter and thickness of solidified shell changes over time during the initial solidification.

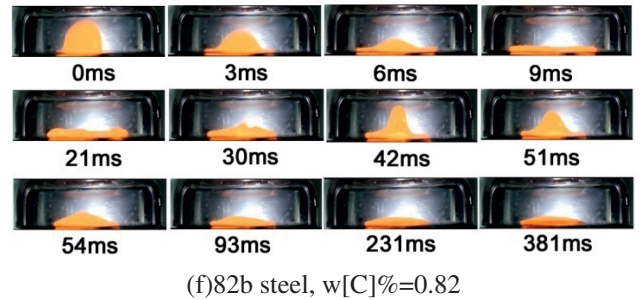
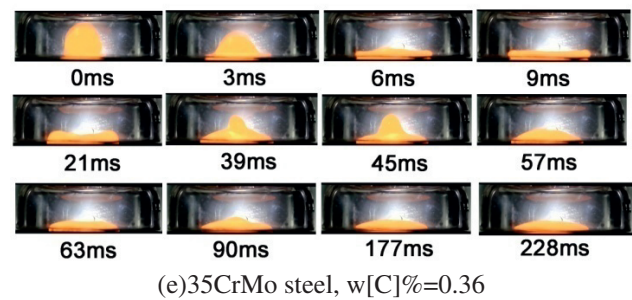
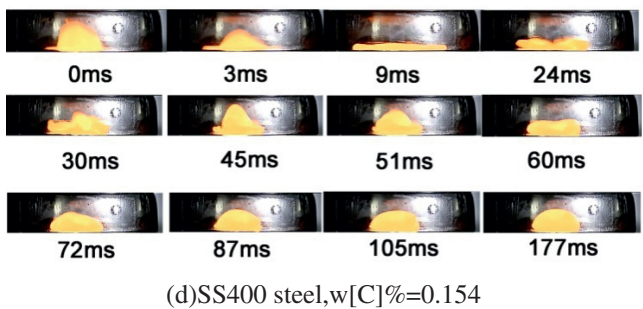
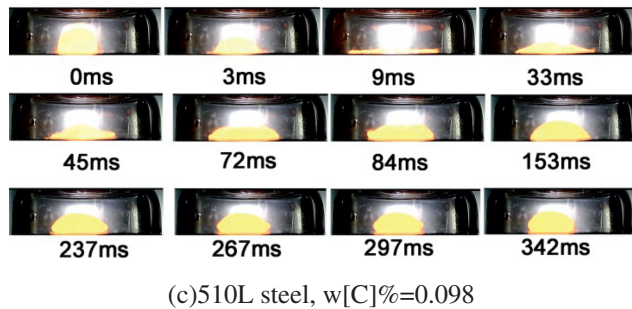
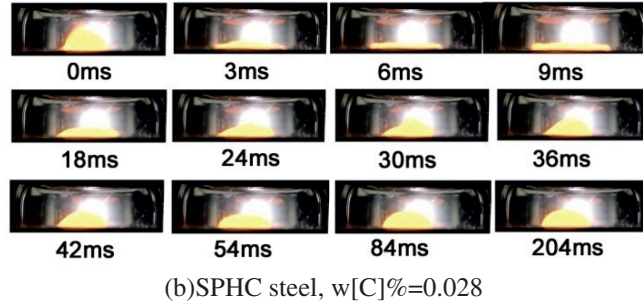
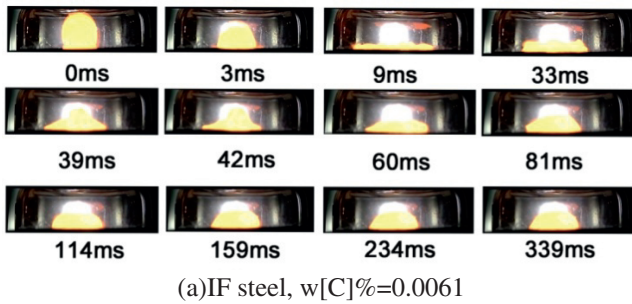


Figure 7: Difference of solidification and deformation of various steels at instant contact of steel droplet and the chill plate.

shell of 35CrMo hyper-peritectic steel and 82b high carbon steel are largest, and that of other steels are the next, and that of 510 L hypo-peritectic steel is smallest. For hypo-peritectic steels, since the shrinkage of solidified shell of 510 L steel (carbon content close to C_B point) is much larger than that of SS400 steel (carbon content close to the C_C point) after completely spread [12], the bottom diameter of solidified shell of 510 L steel is smaller than that of SS400 steel.

The initial solidified shell forms at the meniscus in mold after the contact of molten steel and mold copper plate during continuous casting. At the time of t_s , the solidified shell reaches a critical thickness (Sc) and a certain strength, and begins to deform elastically, then the shell pulls away from mold copper plate to a convex which leading to the formation of air gap [5]. In the initial solidification experiments, the cooling rate of molten steel after the contact with copper chill plate is very large, and there is also a critical thickness of solidified shell, which is similar with that at the meniscus in mold. Take 510 L hypo-peritectic steel for example, the droplet spreads completely to maximum bottom diameter and minimum thickness at the time of 9 ms. The droplet begins to shrink inward with higher thickness at the time of 9–45 ms, which is not totally solidified. At the time of 45 ms, the molten steel contacts with bottom is totally solidified, however, the above molten steel has not been solidified. This is because the top temperature of sample is higher than the bottom temperature, and there is a temperature gradient in the sample. At the time of 72–297 ms, the solidified shell begins to shrink inward with smaller bottom diameter and larger thickness, which appears

spherical. After the time of 297 ms, the sample remains a fixed shape with unchanged diameter and thickness. Compared with other steels, there is a sharply shrinkage at the end of solidification, and the bottom diameter of the solidified shell reduces to very small values linearly.

Difference of bottom deformation degree of solidified shell of various steels

The appearances of solidified shell of various steels formed on the copper chill plate (burnished) were shown in Figure 9. The appearances of solidified shell for high carbon steels and hyper-peritectic steels with high carbon content show lamellar, while that for other steels show spherical. Among them, the appearances of solidified shell for most hypo-peritectic steels are spherical with small bottom diameter. Figure 10 is the average bottom diameter of solidified shell of various steels with different carbon content. It is shown that with the increase of carbon content, the bottom diameter of solidified shell decreases gradually when the carbon content is less than 0.176 %, and the diameter increases until the carbon reaches 0.0514 %, then decreases when the carbon content is more than 0.0514 %. The bottom diameters of solidified shell of low-carbon steels and hypo-peritectic steels are small, and that of high carbon steels and hyper-peritectic steels are large.

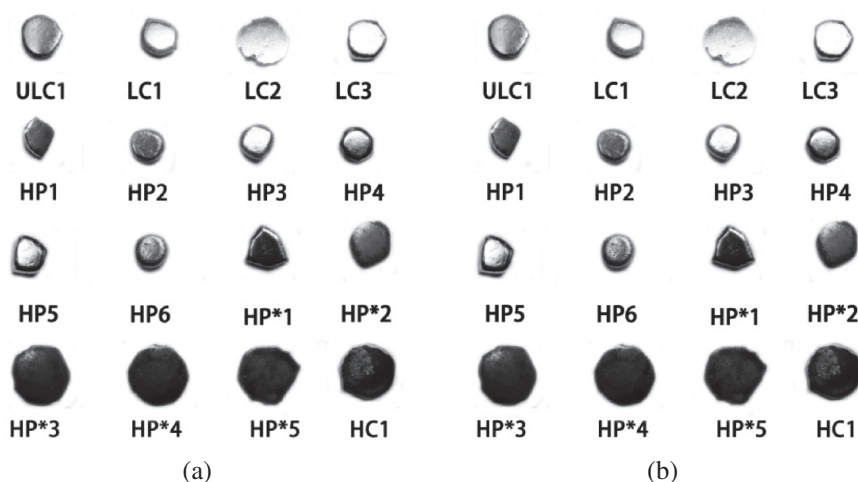


Figure 9: Appearances of solidified shell of various steels, (a) top; (b) bottom.

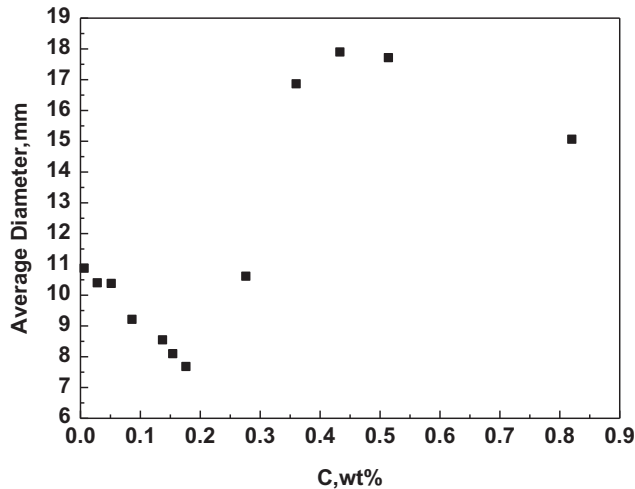


Figure 10: Affect of carbon content on the average bottom diameter of solidified shell.

The bottom profiles of center section of solidified shell of different steels are shown in Figure 11. It is shown that besides the solidified shell of high carbon steel occasionally show negative deformation which is concave towards the chill, that of other steels show positive deformation which is convex towards the chill. The curvature value (κ) changes with the carbon content, and κ is large when the carbon content is in the hypo-peritectic range, which means large deformation degree. The bottom layer of liquid steel solidifies into a thin shell quickly at the transient instant when the droplet contacts with the chill plate. If the bottom thin shell does not stick to the chill plate, the bottom shell is relatively free to shrink without significant stress, and the next layer of liquid steel above the solidified shell then solidifies [13]. Under the combined action of the shrinking stress of solidification and phase transformation, tensile force of liquid steel, and the under layer tends to bend, and the solidified shell is convex towards the chill along with the solidification layer by layer. If the bottom thin shell sticks to the chill plate, because the under layer suffers compressive stress and the above layer suffers tensile stress, the whole solidified shell is concave or planar towards the chill. For ultra-low carbon steel, low carbon steel, hypo-peritectic steel, and hyper-peritectic steel, since the bottom thin shell does not stick to the chill plate due to the narrow liquid-solid phase region, the solidified shells are convex towards the chill. For high-carbon steel, due to the wide liquid-solid phase region, the bottom thin shell tend to stick to the chill plate with compressive stress, and the shrinkage stress is small due to the solidification mode. Thus, the solidified shell of high carbon

steel is convex towards the chill if shrinkage stress is smaller than compressive stress, while that is concave towards the chill if shrinkage stress is larger than compressive stress.

The effect of carbon content ($w[C]\%$) and carbon equivalent content (C_{eq}) on the deformation degree of the solidified shell is shown in Figure 12. It is shown that with higher carbon content, the κ of bottom profile of center section of solidified shell decreases gradually when $0.0061 < w[C]\% \leq 0.0514$ ($0.00446 < C_{eq} \leq 0.0516$), and increases when $0.0514 < w[C]\% \leq 0.082$ ($0.0516 < C_{eq} \leq 0.1016$), then decreases when $w[C]\% > 0.082$ ($C_{eq} > 0.85806$). The change law of deformation degree of solidified shell in droplet experiments conforms with that of growth uniformity of initial solidified shell for various steels during continuous casting, in which the deformation degrees of solidified shell for ultra-low carbon steel and hypo-peritectic steel are large. The root reason of this phenomenon is the difference of solidification mode characteristics of various steel grades, which have high and narrow temperature range of $\delta \rightarrow \gamma$ phase transformation for ultra-low carbon steel and $L + \delta \rightarrow \gamma$ and $\delta \rightarrow \gamma$ phase transformation for hypo-peritectic steel. Figure 12(a) shows that the κ is largest when $w[C]\% = 0.082, 0.098$ ($C_{eq} = 0.1016, 0.12$), which is consistent with Murakami and Sugitani's [14, 15] results (the uneven degree of initial solidified shell in mold is very large when $0.09 < w[C]\% \leq 0.12$, and that is largest when $w[C]\% = 0.1$), and the previous theoretical analysis results [12] (the uneven degree of initial solidified shell is largest for hypo-peritectic steel which $w[C]\%$ near C_B). With comparison of the Figures 10 and 12, it's found that the deformation degree is usually small with the large bottom diameter, which shows an opposite changing direction.

Difference of structure of solidified shell of various steels

Under the equilibrium condition, the microstructures of different steels at room temperature mainly contain F (ultra-low carbon steel), F + P (low carbon steel, hypo-peritectic, and hyper-peritectic steel), Fe₃C + P (high carbon steel). However, since the cooling process of droplet contact with copper chill plate in this experiment is not an equilibrium process, there is great difference between the microstructures of solidified shell and the above equilibrium microstructures. The top and bottom microstructures of center section of solidified shell of various steels observed by metallographic microscope are shown in Table 2. It is shown that the microstructure of solidified

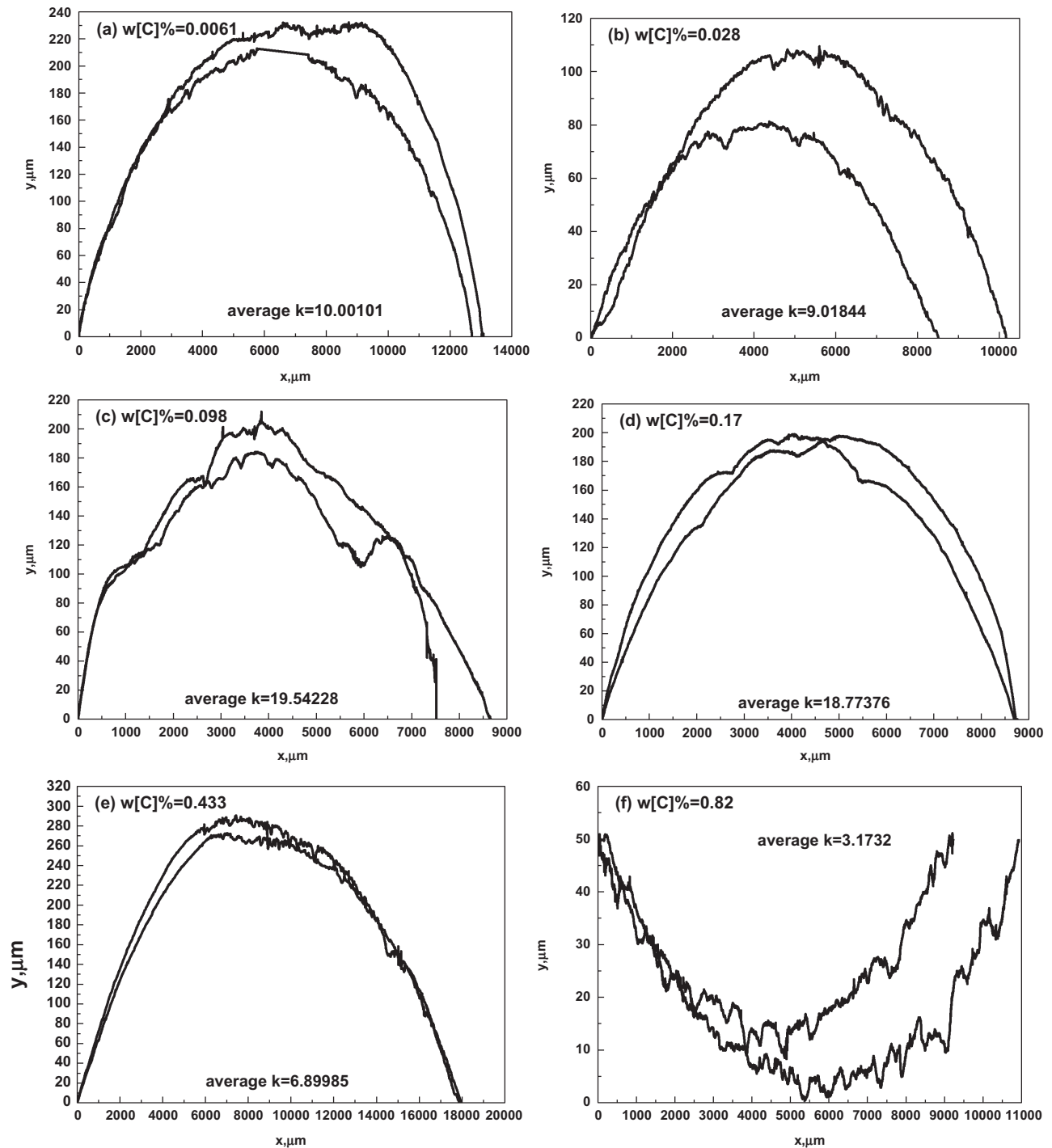


Figure 11: The bottom profiles of center section of solidified shell with different carbon content, (a) ultra-low carbon steel; (b) low carbon steel; (c) hypo-peritectic steel; (d) peritectic steel; (e) hyper-peritectic steel; (f) high carbon steel.

shell of hypo-peritectic steel is bainite, while that of hyper-peritectic steel is martensite, and that of high carbon steel is martensite and little cementite. The grain size of bottom shell is obviously finer than that on top shell.

In addition, the bottom microstructure of solidified shell of hypo-peritectic steel is fine granular bainite, and the top microstructure is grosser featherlike bainite with higher height.

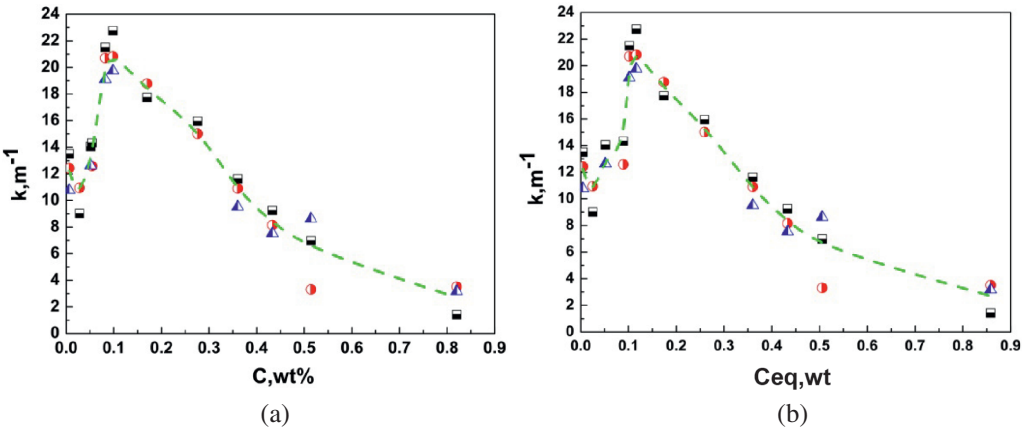


Figure 12: Effect of carbon content on the deformation degree of the solidified shell, (a) actual carbon content ($w[C]\%$); (b) carbon equivalent content (C_{eq}).

Table 2: Metallographic graphs of center section of solidified shell of various steels (4 % nitric acid alcohol erosion).

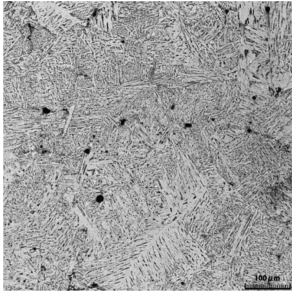
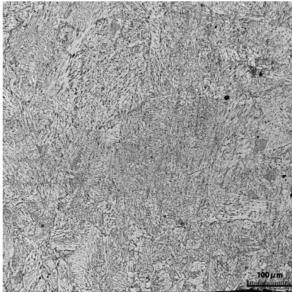
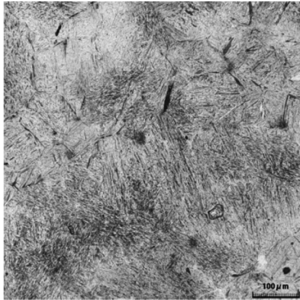

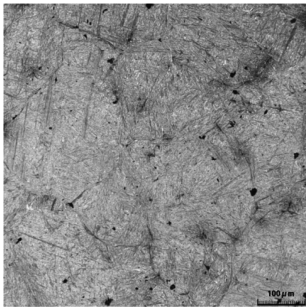
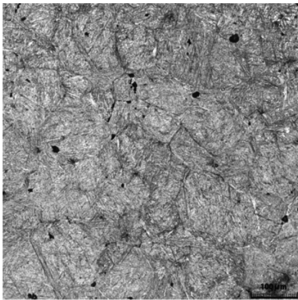
Steel grade	Top	Bottom	Microstructure
510 L hypo-peritectic steel			Bainite
50Mn hyper-peritectic steel			Martensite
82B high carbon steel			Martensite + little cementite

Figure 13 is the macrostructures at different parts of center section of solidified shell of 50 Mn steel. It is shown that the top center macrostructure is bulky columnar crystal, while the bottom center macrostructure is fine columnar crystal. This is because the cooling rate of molten steel on the copper chill plate is much larger than in air, thus the heat transfer of solidified shell on the copper chill plate is approximated as 1-D unidirectional heat transfer

Heat transfer of solidified shell on the copper chill plate of various steels

The heat flux near copper plate surface could be calculated by the finite difference method on the hypothesis that heat transfer of molten steel and copper plate is 1-D unidirectional heat transfer. After deforming the one-dimensional heat conduction equation (3), Formula (4) could be obtained. At the time of j , the copper plate temperature ($T_{0,j}$) could be calculated by formula (5), in which Δx is distance interval (0.002 m), and Δt is time interval (0.003 s). With the change of time, T_1 and T_2 have been measured by T-type thermocouple, and the surface temperature of copper plate (T_0) could be calculated by Formula (5). And the heat flux density of the copper plate surface at the time of j could be calculated by Formula (6).

$$\frac{dT}{dt} = \left(\frac{\kappa}{\rho C_p} \right) \frac{d^2 T}{dx^2} = \left(\frac{\kappa \Delta t}{\rho C_p \Delta x^2} \right) [T_{0,j} - 2T_{1,j} + T_{2,j}] \quad (3)$$

$$T_{1,j+1} = T_{1,j} + \left(\frac{\kappa \Delta t}{\rho C_p \Delta x^2} \right) [T_{0,j} - 2T_{1,j} + T_{2,j}] \quad (4)$$

$$T_{0,j} = (T_{1,j+1} - T_{1,j}) \left(\frac{\rho C_p \Delta x^2}{\kappa \Delta t} \right) + 2T_{1,j} - T_{2,j} \quad (5)$$

$$q_{|x=0,j} = \kappa \frac{dT}{dx}_{|x=0,j} = k \frac{T_{0,j} - T_{1,j}}{\Delta x} \quad (6)$$

When the molten steel ($10^\circ\text{C} < \text{superheat} < 20^\circ\text{C}$, weighing 4 g) of typical steels with different solidification modes dropped, the heat flux density of the copper chill plate surface was shown in Figure 14. It is shown that the heat flux density of copper chill plate has risen sharply at instant contact of steel droplet and the chill plate, and there is a peak of heat flux density of copper chill plate in droplet experiments of all steels before 0.1 s. And the heat

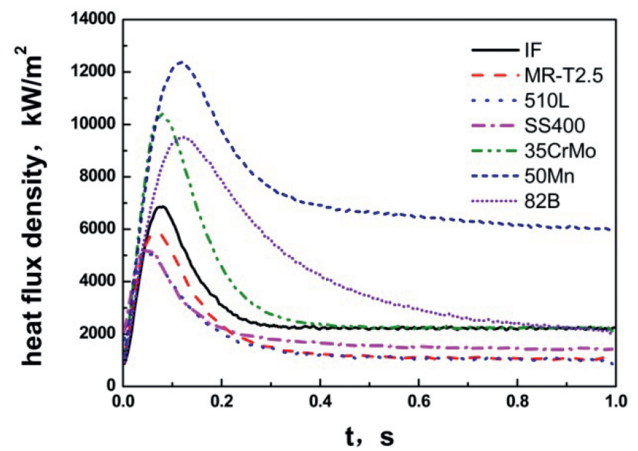
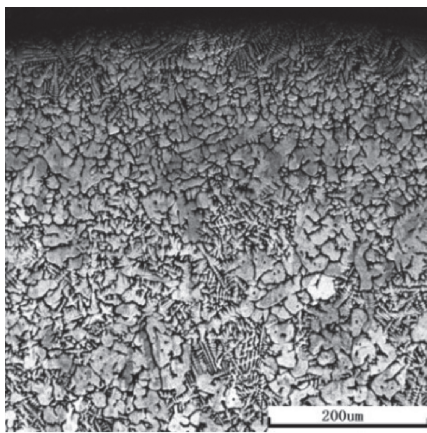
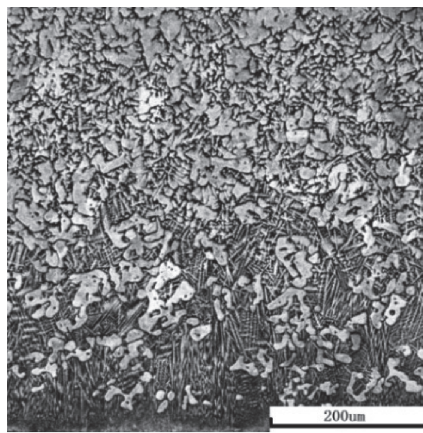


Figure 14: Heat flux density of the copper chill plate changes over time in droplet experiments of various steels.



(a)



(b)

Figure 13: Macrostructures of center section of solidified shell of 50 Mn steel (supersaturated picric acid erosion, 1,000 \times), (a) top center; (b) bottom center.

flux density begins to decrease gradually at the time of 0.1–0.2 s, and slowly decrease to remain stable after 0.2 s. The effect of carbon content on the peak heat flux density is shown in Figure 15. It is shown that the heat flux density of 510 L and SS400 hypo-peritectic steels are relatively low (5,062 kW/m² and 5,288 kW/m²), that of MR-T2.5 low carbon steel and IF ultra-low carbon steel are larger (5,062 kW/m² and 6,768 kW/m²), and that of 82B high carbon steel and 50Mn hyper-peritectic steel are very large (9,514 kW/m² and 12,379 kW/m²). The change law of the peak heat flux density is related to the difference of solidification mode characteristics of various steel grades. For hypo-peritectic steel, there is uneven air gap between the bottom of solidified shell and chill plate, which leading small amount of peak heat flux density of copper chill plate. Since heat flux density is an important index of heat transfer condition at the meniscus range in mold during continuous casting, the growth of initial solidified shell is directly affected. Based on the law of the heat flux density at the initial solidification, good surface quality of slabs would be achieved by aid of modifying mold flux and cooling intensity in the mold.

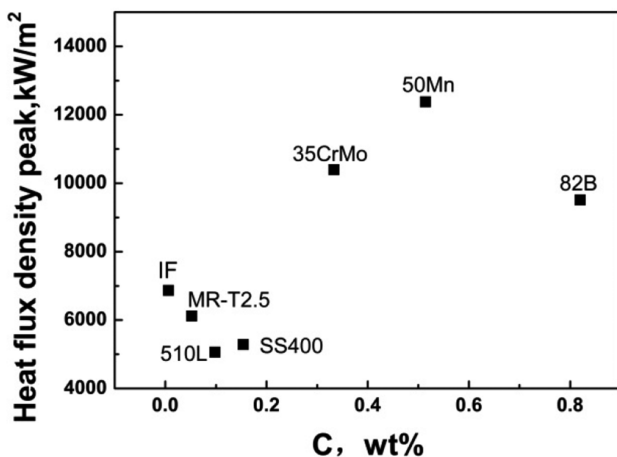


Figure 15: Effect of carbon content on heat flux density peak.

Conclusions

- (1) The appearances of solidified shell of various steels in the droplet experiments are different. The solidified shell of high carbon steels and some hyper-peritectic steels with high carbon content show lamellar, while of other steels show spherical. The profile on the bottom of center section of the solidified shell is a parabola. Besides the solidified

shell of high carbon steels occasionally show negative deformation which is concave towards the chill, that of other steels show positive deformation which is convex towards the chill.

- (2) The deformation degree decreases gradually in order of the hypo-peritectic steel, ultra-low carbon steel, hyper-peritectic steel, low carbon steel, and high carbon steel. Among them, the deformation degree is largest when $w[C]\% = 0.082$. In addition, the deformation of solidified shell gradually decreases with increasing weight and superheat of molten steel.
- (3) The microstructure of solidified shell of hypo-peritectic steel is bainite, while that of hyper-peritectic steel is martensite, and the grain size of bottom shell is obvious finer than that on top shell. The heat flux density of copper chill plate has risen sharply to a peak at instant contact of steel droplet of every steel and the chill plate at about 0.1 s, and then decreases to a certain value after 0.3 s. Compared with other steels, the heat flux density of hypo-peritectic steel is lowest, while that of hyper-peritectic steel is largest.

Funding: This work was funded by National Natural Science Foundation of China (No. 51504172), (No. 51474163), and China Postdoctoral Science Foundation (No. 2015M572212).

References

- [1] M.H. Trejo, E.A. Lopez and J.J.R. Mondragon, *Metals Mater. Int.*, 16 (2010) 731–737.
- [2] K. Matsuura and M. Kudoh, *Metals Mater.*, 4 (1998) 562–565.
- [3] H. Mizukami, A. Yamanaka and T. Watanabe, *ISIJ Int.*, 42 (2002) 964–973.
- [4] V. Guyot, J. Martin and A. Ruelle, *ISIJ Int.*, 36 (1996) S223–S227.
- [5] S.X. Dong, E. Niyama and K. Anzai, *Mater. Trans.*, 35 (1994) 196–198.
- [6] H. Esaka, T. Shirakami and T. Mizoguchi, *Tetsu to Hagané*, 81 (1995) 631–636.
- [7] M. Suzuki and Y. Yamaoka, *Mater. Trans.*, 44 (2003) 836–844.
- [8] H. Mizukami and A. Yamanaka, *ISIJ Int.*, 50 (2010) 435–444.
- [9] S. Dong, E. Niyama and K. Anzai, *ISIJ Int.*, 35 (1995) 730–736.
- [10] M.G. Shen, S.T. Jin and E. Niyama, *Acta Metall. Sinica*, 36 (2000) 1104–1108 ((In Chinese)).
- [11] H. Todoroki and N. Phinichka, *ISIJ Int.*, 49 (2009) 1347–1355.
- [12] Y. Li, X. Zhang and P. Lan, *Int. J. Miner. Metall Mater.*, 20 (2013) 138–145.
- [13] B.G. Thomas, *ISIJ Int.*, 35 (1995) 737–743.
- [14] H. Murakami and M. Suzuki, *Tetsu to Hagané*, 78 (1987) 105–112.
- [15] Y. Sugitani and M. Nakamura, *Tetsu to Hagané*, 65 (1979) 1702–1711.